

Fermi National Accelerator Laboratory

FERMILAB-Conf-90/91-E
[E-741/CDF]

Inclusive Jet Cross Section at $\sqrt{s}=1.8$ TeV *

The CDF Collaboration

presented by

Timothy L. Hessing
Texas A&M University
College Station, Texas 77843

May 1990

* To be published in the proceedings of the XXVth Rencontres de Moriond, High Energy Hadronic Interactions, Les Arcs, Savoie, France, March 11-17, 1990.



Operated by Universities Research Association Inc. under contract with the United States Department of Energy

To be Published in the Proceedings of
the XXV Rencontres de Moriond,
Hadronic Interactions,
March 11-17, 1990
CONF 90/91-E

INCLUSIVE JET CROSS SECTION AT $\sqrt{s} = 1.8 \text{ TeV}$

The CDF Collaboration*
Presented by Timothy L. Hessing
Department of Physics
Texas A&M University, College Station Tx. 77843-4242, USA



Abstract

The inclusive jet cross section at $\sqrt{s} = 1.8 \text{ TeV}$ has been measured at the Fermilab Tevatron Collider. This measurement spans approximately 7 orders of magnitude in cross section and contains jets ranging from 30 GeV to over 400 GeV in transverse energy (E_t). Comparisons have been made to QCD at both order α_s^2 and α_s^3 .

* The collaborating institutions are listed in the Appendix.

Motivation

In the 1988–1989 CDF data run, approximately 4.5 pb^{-1} of data were collected at $\sqrt{s} = 1.8 \text{ TeV}$. The jets in this sample range from 30 GeV to 400 GeV and span 7 orders of magnitude in cross section. Compared to the previously published CDF result¹⁾, QCD can be examined over a much larger range of E_t and the point-like scattering of partons can be probed at distance scales smaller than $5 \times 10^{-17} \text{ cm}$. In addition, order α_s^3 QCD calculations are now available^{2,3)}, which feature a variation of cross section with jet cluster cone size.

Data Selection

The CDF detector has been described in detail elsewhere⁴⁾. Jets in the central pseudorapidity region ($0.1 \leq |\eta| \leq 0.7$), with an event vertex within 60 cm of the center of the detector, were used in this measurement. The data were collected using a single-jet trigger, which formed jets from clusters of energy deposited in the calorimeter. Events were required to contain at least one jet having an E_t above a threshold of 20, 40 or 60 GeV where the 20 and 40 GeV triggers were pre-scaled.

For events passing the trigger requirements, jets were reconstructed using a fixed cone algorithm¹⁾. The cone size (R) is defined by $R = \sqrt{\Delta\eta^2 + \Delta\phi^2}$, where η and ϕ represent the pseudorapidity and azimuthal angle. The trigger efficiency for each cone size (0.4, 0.7 and 1.0) was determined by comparisons of the data from the different triggers in the regions where they overlapped. To eliminate trigger threshold effects, cuts were imposed on jet E_t , to insure $\sim 100\%$ efficiency.

Cosmic rays, which can deposit significant amounts of energy by bremsstrahlung, were removed from this sample in two ways. Cosmic rays, not in coincidence with the beam-beam crossing, were removed using timing information in the hadron calorimeter. The remaining events, containing at least one jet with $E_t \geq 150 \text{ GeV}$, were scanned. From this scanning, events were then rejected on the basis of: the average electromagnetic fraction of the jets in the event, the average Charge/Total energy for central jets, the missing E_t of the event. The estimated contamination after these cuts is $\leq 1\%$ for jets with $E_t \geq 150 \text{ GeV}$.

Jet Energy Response

The effects of resolution smearing and energy degradation due to calorimeter non-linearities, uninstrumented regions of detector, etc. can distort the measured E_t distribution. In order to correct the cross section for these effects, a detector simulation was used. It was tuned to reproduce the single pion response observed in the test beam and the jet fragmentation

observed in the data.

The response of the detector to jets was extracted from the simulation. This response function was used in the unsmearing procedure to correct the data. Corrections for energy loss outside the cone of the jet were not applied in order to be able to compare the next-to-leading order (α_s^3) QCD calculations. When comparing to leading order (α_s^2) QCD calculations, for which an out-of-cone energy correction would be appropriate, this may have some effect.

The unsmearing procedure combines the effects of a falling E_t spectrum and the response function obtained from the tuned simulation. The procedure starts with a parameterized curve and smears this with the response function. The resulting smeared curve is then binned in the same way the data is binned and the result is compared to the data. Using the χ^2 formed between the smeared curve and the data, the parameters in the initial curve are tuned until the χ^2 is minimized. The information from the resulting smeared curve and the input curve are then used to unsmear and correct the data.

Systematic Uncertainties

The major sources of systematic uncertainty on the jet energy scale results from uncertainty on calorimeter response, the fragmentation tuning, and energy from the underlying event (within the cone). The dominant uncertainty in the response for jets containing pions with energies less than 25 GeV comes from the uncertainty in the low energy response. For jets containing pions with energies greater than 25 GeV , the dominant uncertainty comes from the modeling of the response in the azimuthal boundary regions between calorimeter cells. The overall tuning of the fragmentation is in good agreement with the data. The uncertainty in the fragmentation tuning is correlated with the tracking efficiency. The uncertainty in the tracking efficiency for tracks in the cone of the jet was found to be $\pm 7\%$. This uncertainty was varied, within these limits, in the simulation to give a corresponding uncertainty on the energy scale. Finally, due to differences in the definition of the underlying event, there is a $\sim 540 MeV$ uncertainty in the underlying event contribution to a cone of 0.7. Adding all these uncertainties in quadrature, the overall systematic uncertainty on the jet energy scale varies from $\sim 4\%$ at 20 GeV to $\sim 3\%$ for energies in excess of 100 GeV . The uncertainty in the RMS width of the response was obtained by comparing the results of balancing the E_t in two-jet events for the data and simulation. From this comparison a conservative 8% uncertainty on the jet resolution was assigned. Finally, an overall 15% systematic uncertainty is assigned to the measurement of the luminosity.

Results

The resulting cross section for cone sizes of 0.4, 0.7 and 1.0 can be found in Tables 1a-c. Figure 1 shows the cross section for a cone size of 0.7 compared to a leading order QCD calculation. The QCD calculation was normalized to the data by minimizing the χ^2 between the data and the QCD calculation in a limited range of E_t (in figure 1 we choose to use the range from 80 to 160 GeV). The reason for normalizing in a limited region of E_t , is due to the fact that QCD and compositeness will agree in shape over some range of E_t and disagree elsewhere. Therefore in order to search for compositeness, the predictions are normalized in a region where they agree and the data is then compared to the predictions in the region where the predictions disagree. A slight excess of events at the high E_t end can be seen in figure 1. The statistical level of this excess, however, is only 2.5 to 3.5 standard deviations.

Figure 2 shows the same cross section now compared to next-to-leading order QCD, where the QCD normalization is absolute. A comparison is also made to next-to-leading order QCD in figure 3, which shows the cross section as a function of cone size for 100 GeV E_t jets. The data, in these figures, appears to be consistent with both leading and next-to-leading order QCD.

Also shown in figure 3 is the ratio of the cross sections, for different cone sizes, to the cross section for jets with a cone size of 0.7. This shows the data appears to have a steeper variation as a function of cone size, than α^3 calculations would predict. The data and associated statistical errors for figure 3 can be found in Tables 2a-b. Bin to bin correlations of the systematic uncertainties are under study, therefore the systematic uncertainties have not been listed in the tables or shown in the figures.

Summary

The inclusive jet cross section at $\sqrt{s} = 1.8 TeV$ has been measured in the E_t range from 30 to 420 GeV , spanning 7 orders of magnitude. Investigations of the dependence of jet cross section with cone size are in progress. The data appears to be consistent with both leading and next-to-leading order QCD for the structure functions examined, with a small excess of events observed, at high E_t , over leading order QCD predictions. Correlations in the systematic uncertainties are under study. Based on previous studies, we can set a lower limit of 950 GeV (95% C.L.) for the quark compositeness scale parameter Λ^* ⁵⁾, associated with an effective contact interaction. Work is in progress to extract a final cross section and composite limit.

Appendix

Argonne National Laboratory — Brandeis University — University of Chicago — Fermi National Accelerator Laboratory — Laboratori Nazionali di Frascati of the Istituto Nazionale di Fisica Nucleare — Harvard University — University of Illinois — National Laboratory for High Energy Physics (KEK) — Lawrence Berkeley Laboratory — University of Pennsylvania — Istituto Nazionale di Fisica Nucleare, University and Scuola Normale Superiore of Pisa — Purdue University — Rockefeller University — Rutgers University — Texas A&M University — University of Tsukuba — University of Wisconsin

References

- [1] CDF Collaboration, F. Abe, *et al.* Phys. Rev. Lett., **62** (1989) 613.
- [2] S.D. Ellis, Z. Kunszt and D.E. Soper, ETH-TH/90-3 (1990).
- [3] F. Aversa, *et al.* LNF-90/012 PT (1990).
- [4] CDF Collaboration, Nucl. Instr. and Meth. **A267**, 249, 257, 272, 280, 301, 315, 330; **A268** 24, 33, 41, 46, 50, 75, 92 (1988).
- [5] CDF Collaboration, Presented by S. Bertolucci. Proceedings 8th Topical Workshop on $p\bar{p}$ Collider Physics, Castiglione, Italy, September 1, 1989

Table 1a. (CDF PRELIMINARY)		
Inclusive Jet Cross Section at $\sqrt{s} = 1.8 \text{ TeV}$ for Cone Size = 0.4		
$E_t(\text{GeV})$	Cross Section (nb/GeV)	Statistical Error
36.2	$0.817 \times 10^{+2}$	$\pm 0.011 \times 10^{+2}$
41.9	$0.395 \times 10^{+2}$	$\pm 0.007 \times 10^{+2}$
47.5	$0.196 \times 10^{+2}$	$\pm 0.005 \times 10^{+2}$
53.3	$0.110 \times 10^{+2}$	$\pm 0.004 \times 10^{+2}$
59.0	$0.654 \times 10^{+1}$	$\pm 0.009 \times 10^{+1}$
64.5	$0.401 \times 10^{+1}$	$\pm 0.007 \times 10^{+1}$
69.9	$0.248 \times 10^{+1}$	$\pm 0.006 \times 10^{+1}$
75.3	$0.168 \times 10^{+1}$	$\pm 0.005 \times 10^{+1}$
80.6	$0.115 \times 10^{+1}$	$\pm 0.004 \times 10^{+1}$
85.8	$0.762 \times 10^{+0}$	$\pm 0.031 \times 10^{+0}$
91.1	$0.537 \times 10^{+0}$	$\pm 0.026 \times 10^{+0}$
96.3	$0.410 \times 10^{+0}$	$\pm 0.022 \times 10^{+0}$
101.6	$0.276 \times 10^{+0}$	$\pm 0.003 \times 10^{+0}$
106.9	$0.204 \times 10^{+0}$	$\pm 0.003 \times 10^{+0}$
112.1	$0.157 \times 10^{+0}$	$\pm 0.003 \times 10^{+0}$
117.3	$0.110 \times 10^{+0}$	$\pm 0.002 \times 10^{+0}$
122.7	0.861×10^{-1}	$\pm 0.019 \times 10^{-1}$
127.9	0.650×10^{-1}	$\pm 0.017 \times 10^{-1}$
133.1	0.494×10^{-1}	$\pm 0.015 \times 10^{-1}$
138.3	0.395×10^{-1}	$\pm 0.013 \times 10^{-1}$
143.5	0.327×10^{-1}	$\pm 0.012 \times 10^{-1}$
148.8	0.268×10^{-1}	$\pm 0.011 \times 10^{-1}$
153.9	0.188×10^{-1}	$\pm 0.009 \times 10^{-1}$
159.1	0.152×10^{-1}	$\pm 0.008 \times 10^{-1}$
166.9	0.121×10^{-1}	$\pm 0.005 \times 10^{-1}$
177.0	0.755×10^{-2}	$\pm 0.041 \times 10^{-2}$
187.5	0.456×10^{-2}	$\pm 0.032 \times 10^{-2}$
198.2	0.260×10^{-2}	$\pm 0.024 \times 10^{-2}$
210.4	0.178×10^{-2}	$\pm 0.016 \times 10^{-2}$
227.2	0.107×10^{-2}	$\pm 0.013 \times 10^{-2}$
241.4	0.535×10^{-3}	$\pm 0.091 \times 10^{-3}$
259.3	0.429×10^{-3}	$\pm 0.081 \times 10^{-3}$
277.5	0.301×10^{-3}	$\pm 0.059 \times 10^{-3}$
299.2	0.926×10^{-4}	$+0.458 \times 10^{-4} - 0.321 \times 10^{-4}$
317.6	0.693×10^{-4}	$+0.416 \times 10^{-4} - 0.276 \times 10^{-4}$
338.9	0.346×10^{-4}	$+0.338 \times 10^{-4} - 0.188 \times 10^{-4}$
371.1	0.232×10^{-4}	$+0.227 \times 10^{-4} - 0.127 \times 10^{-4}$
409.2	0.104×10^{-4}	$+0.138 \times 10^{-4} - 0.067 \times 10^{-4}$

Table 1b. (CDF PRELIMINARY)		
Inclusive Jet Cross Section at $\sqrt{s} = 1.8 \text{ TeV}$ for Cone Size = 0.7		
$E_t(\text{GeV})$	Cross Section (nb/GeV)	Statistical Error
41.6	$0.728 \times 10^{+2}$	$\pm 0.010 \times 10^{+2}$
47.6	$0.349 \times 10^{+2}$	$\pm 0.007 \times 10^{+2}$
53.5	$0.189 \times 10^{+2}$	$\pm 0.005 \times 10^{+2}$
59.9	$0.986 \times 10^{+1}$	$\pm 0.035 \times 10^{+1}$
66.2	$0.589 \times 10^{+1}$	$\pm 0.027 \times 10^{+1}$
72.3	$0.354 \times 10^{+1}$	$\pm 0.006 \times 10^{+1}$
78.2	$0.234 \times 10^{+1}$	$\pm 0.005 \times 10^{+1}$
83.8	$0.168 \times 10^{+1}$	$\pm 0.004 \times 10^{+1}$
89.3	$0.110 \times 10^{+1}$	$\pm 0.004 \times 10^{+1}$
94.8	$0.769 \times 10^{+0}$	$\pm 0.030 \times 10^{+0}$
100.2	$0.540 \times 10^{+0}$	$\pm 0.025 \times 10^{+0}$
105.6	$0.402 \times 10^{+0}$	$\pm 0.022 \times 10^{+0}$
111.0	$0.302 \times 10^{+0}$	$\pm 0.019 \times 10^{+0}$
116.4	$0.206 \times 10^{+0}$	$\pm 0.003 \times 10^{+0}$
121.8	$0.156 \times 10^{+0}$	$\pm 0.003 \times 10^{+0}$
127.1	$0.115 \times 10^{+0}$	$\pm 0.002 \times 10^{+0}$
132.5	0.870×10^{-1}	$\pm 0.019 \times 10^{-1}$
137.8	0.669×10^{-1}	$\pm 0.017 \times 10^{-1}$
143.1	0.519×10^{-1}	$\pm 0.015 \times 10^{-1}$
148.5	0.414×10^{-1}	$\pm 0.013 \times 10^{-1}$
153.7	0.323×10^{-1}	$\pm 0.012 \times 10^{-1}$
158.9	0.266×10^{-1}	$\pm 0.011 \times 10^{-1}$
164.2	0.206×10^{-1}	$\pm 0.009 \times 10^{-1}$
171.9	0.155×10^{-1}	$\pm 0.006 \times 10^{-1}$
182.2	0.104×10^{-1}	$\pm 0.005 \times 10^{-1}$
193.0	0.617×10^{-2}	$\pm 0.037 \times 10^{-2}$
203.5	0.346×10^{-2}	$\pm 0.028 \times 10^{-2}$
215.7	0.241×10^{-2}	$\pm 0.019 \times 10^{-2}$
231.9	0.148×10^{-2}	$\pm 0.015 \times 10^{-2}$
246.9	0.849×10^{-3}	$\pm 0.113 \times 10^{-3}$
264.9	0.442×10^{-3}	$\pm 0.082 \times 10^{-3}$
282.0	0.358×10^{-3}	$\pm 0.064 \times 10^{-3}$
302.2	0.186×10^{-3}	$+0.059 \times 10^{-3} - 0.046 \times 10^{-3}$
322.9	0.816×10^{-4}	$+0.440 \times 10^{-4} - 0.302 \times 10^{-4}$
343.9	0.584×10^{-4}	$+0.397 \times 10^{-4} - 0.253 \times 10^{-4}$
380.7	0.237×10^{-4}	$+0.231 \times 10^{-4} - 0.129 \times 10^{-4}$
418.5	0.975×10^{-5}	$+1.292 \times 10^{-5} - 0.631 \times 10^{-5}$

Table 1c. (CDF PRELIMINARY)		
Inclusive Jet Cross Section at $\sqrt{s} = 1.8 \text{ TeV}$ for Cone Size = 1.0		
$E_t(\text{GeV})$	Cross Section (nb/GeV)	Statistical Error
45.8	$0.524 \times 10^{+2}$	$\pm 0.011 \times 10^{+2}$
53.8	$0.235 \times 10^{+2}$	$\pm 0.006 \times 10^{+2}$
61.3	$0.123 \times 10^{+2}$	$\pm 0.004 \times 10^{+2}$
68.1	$0.667 \times 10^{+1}$	$\pm 0.030 \times 10^{+1}$
74.6	$0.431 \times 10^{+1}$	$\pm 0.024 \times 10^{+1}$
80.4	$0.239 \times 10^{+1}$	$\pm 0.005 \times 10^{+1}$
86.5	$0.171 \times 10^{+1}$	$\pm 0.005 \times 10^{+1}$
92.8	$0.116 \times 10^{+1}$	$\pm 0.004 \times 10^{+1}$
98.7	$0.820 \times 10^{+0}$	$\pm 0.031 \times 10^{+0}$
104.3	$0.559 \times 10^{+0}$	$\pm 0.026 \times 10^{+0}$
109.9	$0.416 \times 10^{+0}$	$\pm 0.022 \times 10^{+0}$
115.5	$0.301 \times 10^{+0}$	$\pm 0.019 \times 10^{+0}$
120.9	$0.220 \times 10^{+0}$	$\pm 0.016 \times 10^{+0}$
126.2	$0.163 \times 10^{+0}$	$\pm 0.003 \times 10^{+0}$
131.6	$0.121 \times 10^{+0}$	$\pm 0.002 \times 10^{+0}$
137.0	0.935×10^{-1}	$\pm 0.020 \times 10^{-1}$
142.4	0.703×10^{-1}	$\pm 0.017 \times 10^{-1}$
147.8	0.542×10^{-1}	$\pm 0.015 \times 10^{-1}$
153.1	0.467×10^{-1}	$\pm 0.014 \times 10^{-1}$
158.5	0.351×10^{-1}	$\pm 0.012 \times 10^{-1}$
163.9	0.281×10^{-1}	$\pm 0.011 \times 10^{-1}$
171.7	0.205×10^{-1}	$\pm 0.007 \times 10^{-1}$
182.2	0.140×10^{-1}	$\pm 0.006 \times 10^{-1}$
193.1	0.835×10^{-2}	$\pm 0.043 \times 10^{-2}$
203.4	0.487×10^{-2}	$\pm 0.033 \times 10^{-2}$
216.4	0.318×10^{-2}	$\pm 0.022 \times 10^{-2}$
233.1	0.189×10^{-2}	$\pm 0.017 \times 10^{-2}$
247.5	0.108×10^{-2}	$\pm 0.013 \times 10^{-2}$
264.6	0.558×10^{-3}	$\pm 0.092 \times 10^{-3}$
282.0	0.467×10^{-3}	$\pm 0.073 \times 10^{-3}$
305.4	0.216×10^{-3}	$+0.062 \times 10^{-3} - 0.049 \times 10^{-3}$
326.5	0.102×10^{-3}	$+0.047 \times 10^{-3} - 0.033 \times 10^{-3}$
348.6	0.450×10^{-4}	$+0.358 \times 10^{-4} - 0.216 \times 10^{-4}$
377.4	0.451×10^{-4}	$+0.271 \times 10^{-4} - 0.179 \times 10^{-4}$
427.8	0.181×10^{-4}	$+0.144 \times 10^{-4} - 0.087 \times 10^{-4}$

Table 2a. (CDF PRELIMINARY)		
Cross Section vs Cone Size at 100 GeV		
Cone Size	Cross Section (<i>nb/GeV</i>)	Statistical Error
1.0	0.759	± 0.025
0.7	0.548	± 0.024
0.4	0.318	± 0.007

Table 2b. (CDF PRELIMINARY)		
Cross Section Ratio vs Cone Size at 100 GeV		
Cone Size	Cross Section (<i>nb/GeV</i>)	Statistical Error
1.0	1.386	± 0.076
0.7	1.000	± 0.063
0.4	0.580	± 0.029

Inclusive Jet Cross Section (Cone Size 0.7)

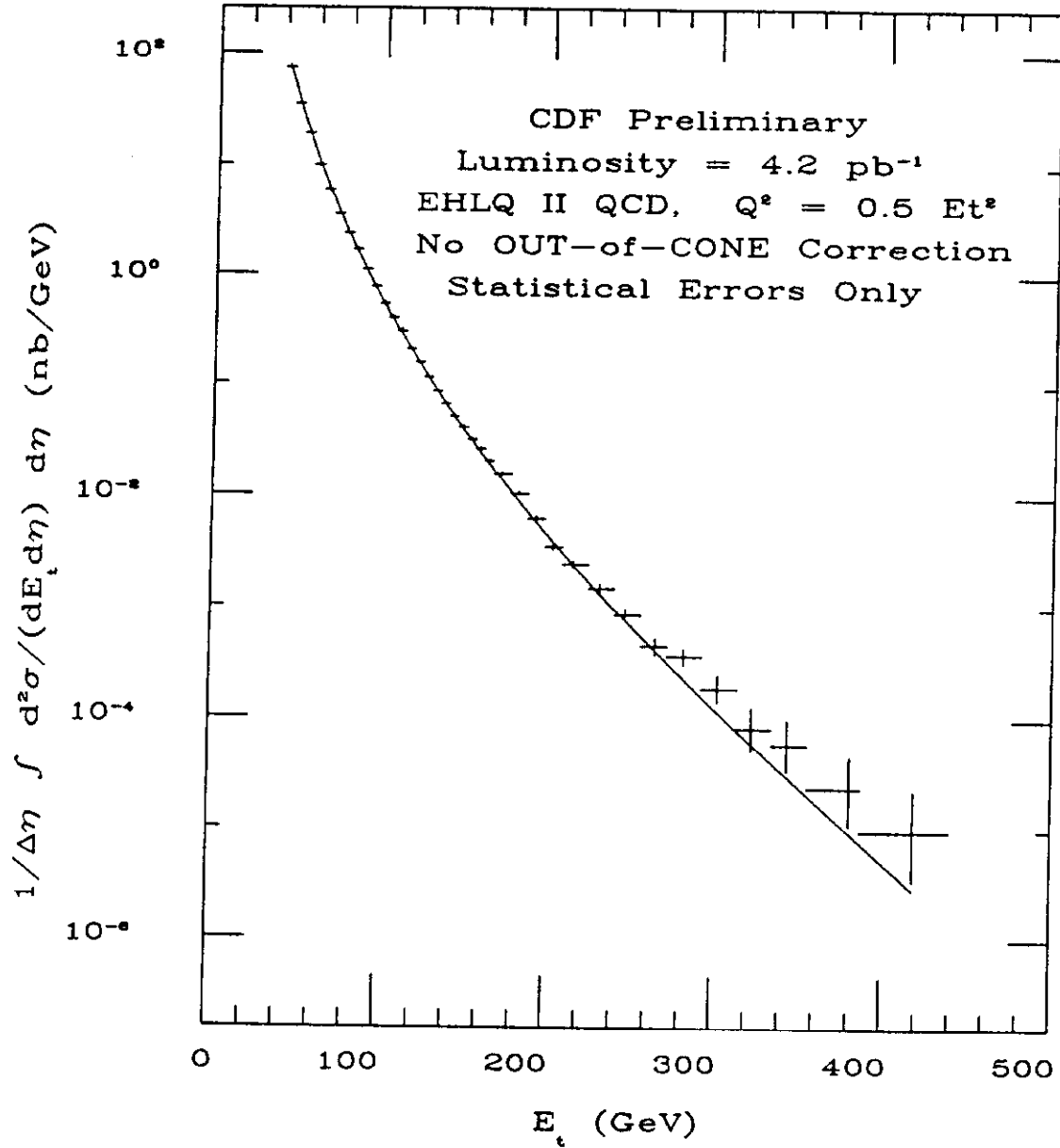


Figure 1: The cross section is compared to a leading order QCD calculation, which uses EHLQ II structure functions and has been normalized to the data in the E_t range from 80 to 160 GeV.

Inclusive Jet Cross Section (Cone Size 0.7)

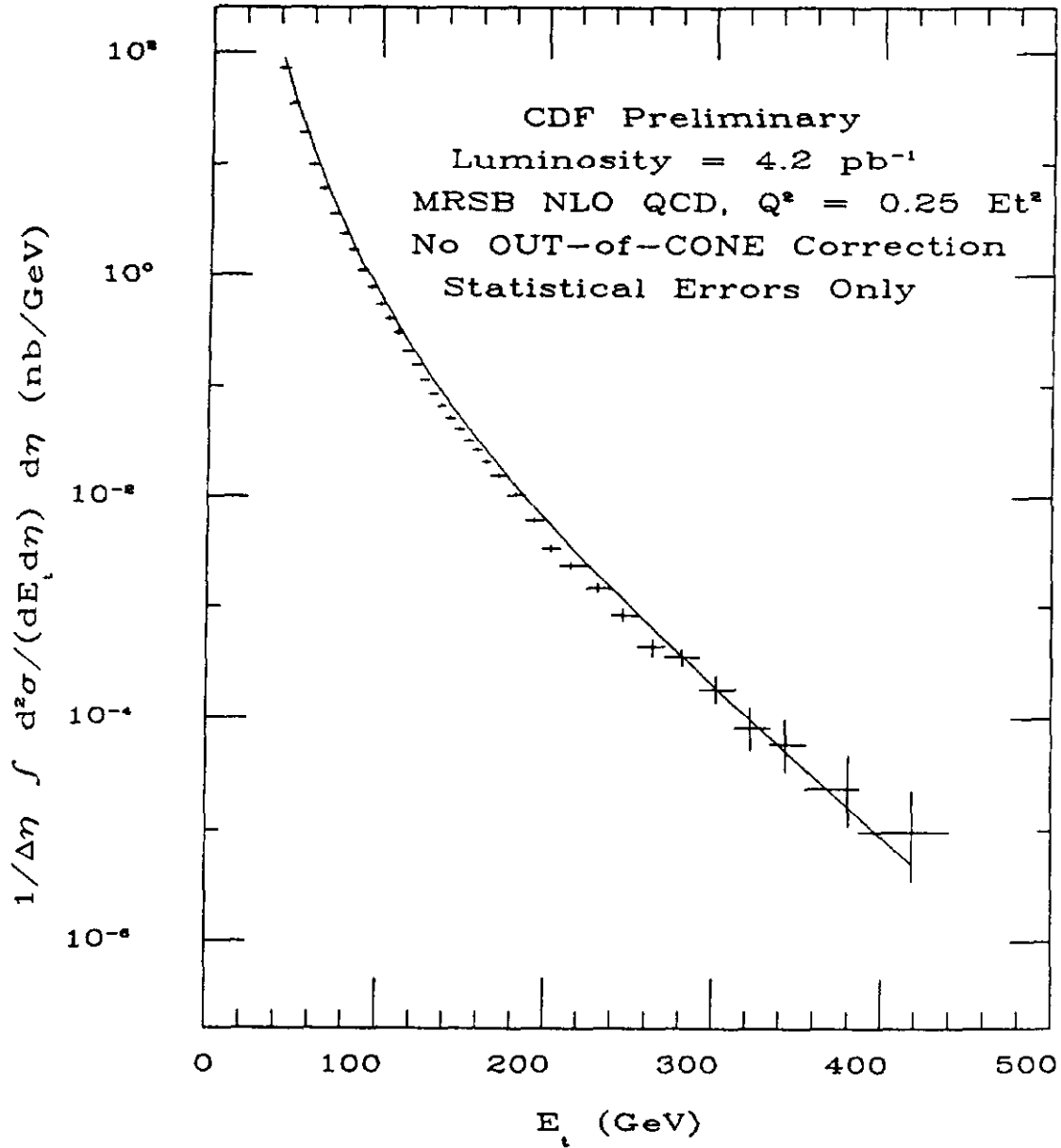


Figure 2: The cross section is compared to next-to-leading order QCD, which uses MRSB structure functions. The normalization is absolute.

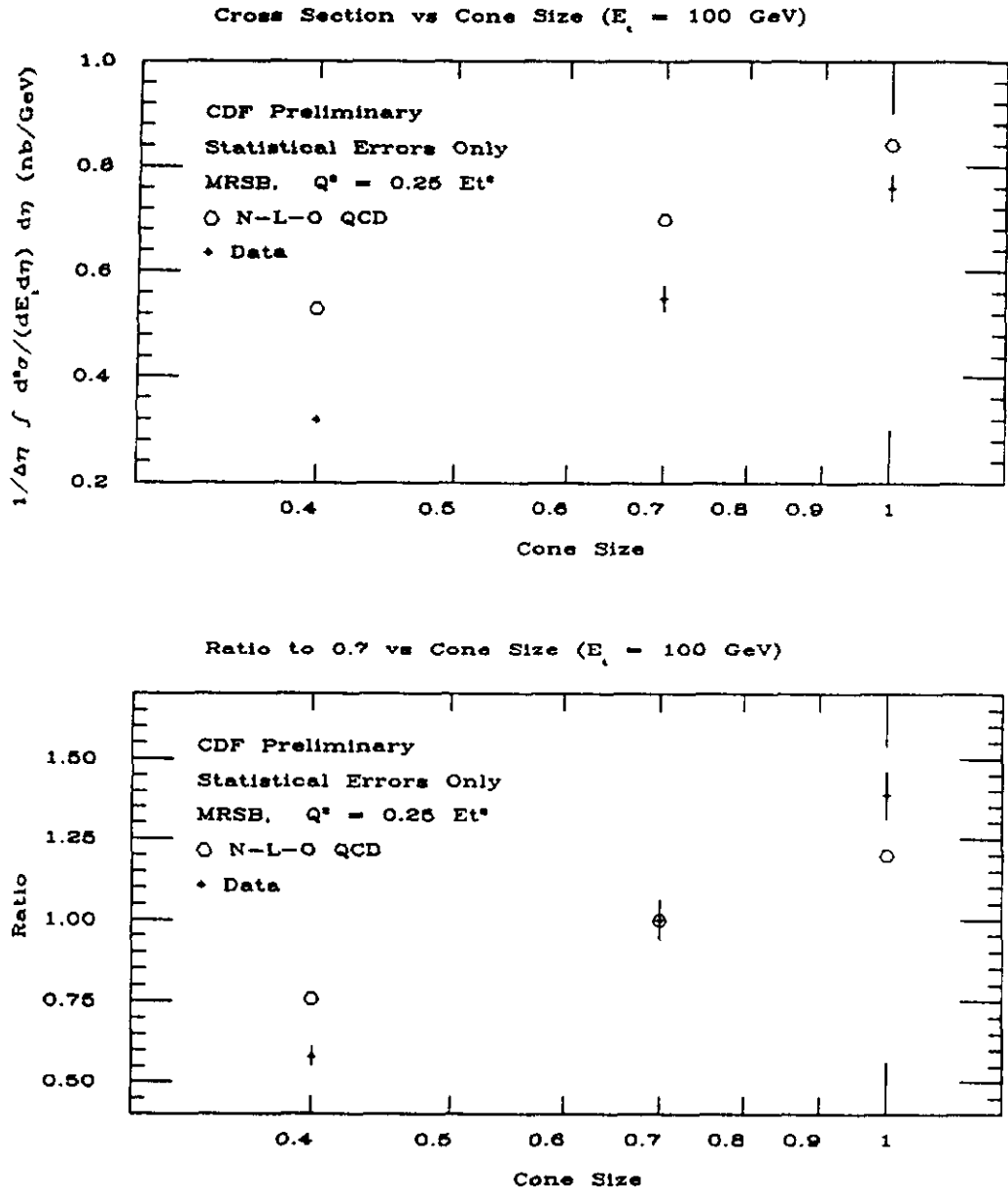


Figure 3: The top plot is the jet cross section for jets with E_t of 100 GeV as a function of cone size compared to next-to-leading order QCD. The bottom plot is the ratio of the cross sections to the cross section for 100 GeV jets with a cone size of 0.7, again compared to next-to-leading order QCD.